Secondary Reflector and Receiver Positions for Uniform Heat Flux Distribution in Parabolic Trough Solar Thermal Collector

Baiju V
Energy Research Lab,
Department of Mechanical Engineering,
TKM College of Engineering,
Kollam, Kerala 691505, India
e-mail: baiju@tkmce.ac.in

Shajan S[1]
Energy Research Lab,
Department of Mechanical Engineering,
TKM College of Engineering,
Kollam, Kerala 691505, India;
APJ Abdul Kalam Technological University,
Kerala 695017, India
e-mail: shajan@sctce.ac.in

The distributions of heat flux over the circumference of the receiver tubes have an immense influence on the performance and reliability of the parabolic trough solar thermal collectors. The location of the receiver tube and the secondary reflector configuration may largely influence the performance of the system. Therefore, in this study, the effect of receiver tube position and parabolic secondary reflector configuration has been analyzed, and the non-uniformity of solar flux distribution, heat gradient, and power output has been compared. The results of the Monte Carlo ray-tracing analysis to homogenize the receiver tube flux distribution and maximize the output power, making the use of the cutting edge solar optical simulation tool Tonatiuh, has been presented. A parabolic trough collector with a rim angle of 80 deg and aperture area of 40 m^2 have been used for the analysis. It has been confirmed that the circumferential heat flux gradient and the local hot spot could be greatly diminished, while the power output tended to reduce slightly due to the shading effect of the secondary reflector. Under the conditions investigated in this work, although the output power decreased by 4.83%, flux gradient reduced significantly, and the non-uniformity of flux distribution has reduced from 0.9757 to 0.5176. A simple design procedure for receiver tube position and secondary reflector configurations to homogenize the receiver tube temperature distribution has also been proposed.
[DOI: 10.1115/1.4054660]

Keywords: parabolic trough collector, secondary reflector, non-uniform heat flux, solar energy, ray-tracing, clean energy, heat transfer, simulation, solar receiver, thermal power

1 Introduction

Fossil fuels contribute severe widespread effects to our climate, as their burning emits greenhouse gases and airborne pollutants. Therefore, an accelerated shift to renewable energy becomes crucial to meet the International Energy Agency's (IEA) sustainable development scenario share of almost half of the generation by 2030. Solar energy is the richest source of renewable energy on the Earth, with an energy density of about 1368 W/m^2 [1]. Parabolic trough collectors (PTC) are one of the most proven and lowest costs concentrated solar power (CSP) technology available today, used in the power generation industry. As shown in Fig. 1, the direct normal irradiance (DNI) fall on the parabolic collector is reflected on the receiver tube, which is located along the focal axis of the concentrator [2]. Heat is then transferred to the heat transfer fluid (HTF), flowing through this receiver.

From Fig. 1, it can be observed that the lower circumference of the receiver tube is exposed to concentrated solar flux, whereas the upper half receives only direct beam radiations. The primary ongoing issue of the receiver tube is the peak heat flux and uneven distribution of solar flux over its circumference that can lead to high-temperature gradient within the receiver tube and flow region [3,4]. The uneven heat flux distribution over the receiver tube is a major issue that initiates some problems such as two-phase fluid inflow channels and thermal deformation of the receiver tube [5,6]. The majority of PTC failures reported are due to the induced stresses and bending of the receivers due to the uneven expansion of the tubes with this non-uniform heat flux distribution [7,8]. Uniformity is defined as the ratio of the standard deviation of the flux distribution to its mean value. A minimum value represents a more uniform heat flux, while a larger value represents a non-uniform value. The solar flux distribution coefficient variation is expressed as non-uniformity [9].

Many researchers attempted to resolve this problem with a focus on the thermal energy conversion enhancements between the receiver tube and HTF [10]. The results of various geometry modifications to the receiver tube showed improved heat transfer along with a reduced temperature gradient. Jaramillo et al. [11] investigated the presence of a twisted tape inside the flow to enhance the heat exchange between the receiver and HTF. Bellos et al. [12] enhanced the heat transfer rate by establishing higher turbulence in the flow with a designed sine wavy insert. Huang et al. [13] succeeded in analyzing the comparison between different receiver geometry modifications, such as dimples, protrusions, and helical fins, for improving the heat transfer in PTC receiver tubes. Ravi Kumar and Reddy [14], as well as Wang et al. [15], conducted experimental studies on the utilization of a porous disc absorber, and their findings revealed a significant increase in performance with a significant pressure drop. Cheng et al. [16] adopted a unilateral multi-longitudinal vortex enhanced receiver design to increase the thermal efficiency while avoiding the local hot spots and temperature gradient on the circumference. The foremost

[1]Corresponding author.

Contributed by the Solar Energy Division of ASME for publication in the Journal of Solar Energy Engineering: Including Wind Energy and Building Energy Conservation. Manuscript received January 3, 2021; final manuscript received May 1, 2022; published online June 20, 2022. Assoc. Editor: Peiwen Li.

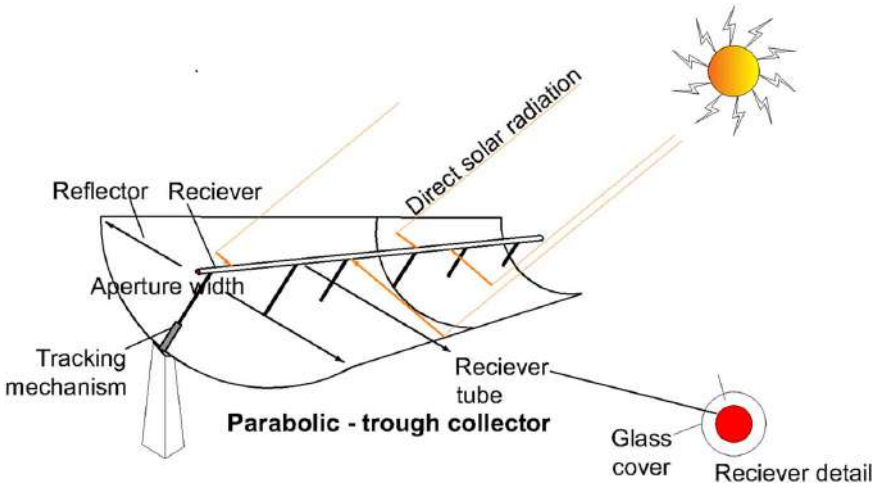

Fig. 1 Schematic of a PTC

reasons for the thermal improvements seen in the geometry modifications of the receiver tube are due to the development of turbulence and swirls in the flow path [17].

Advanced HTFs appear to be one of the most effective methods to enhance solar collectors' thermal performance, and various HTFs have been tested in the literature. Many studies on HTFs in PTCs have shown better heat flux distribution and reduced peak temperatures with improved thermal performance [18–20]. Currently, thermal oils are the most common HTFs for the majority of concentrated solar thermal power plants around the world [21–23]. They can deliver energy up to 400 °C with comparatively much higher efficiency and are a preferred choice over water to withstand high pressure [2]. Xu et al. [20] developed a one-dimensional transient model to compare the thermal response of the PTC receiver with solar salt and therminol oil. Chang et al. [21] and many others analyzed the enhanced heat transfer characteristics of molten salt in a PTC absorber because of its high working temperature (>1100 °C), higher specific heat capacity, and low cost. Their findings showed that the molten salt has a much longer response delay concerning DNI and flowrates than the synthetic oil. One of the most effective ways to improve the thermal performance of solar thermal energy systems is to replace working fluids with nanofluids. Nanoparticles with different desirable thermal characteristics can be used as a better HTF [24]. Kasaeian et al. [23] conducted an investigation of a PTC with multi-walled carbon nanotubes (MWCNT)/mineral oil-based nanofluid as the HTF. Their experimental results showed a 7% global efficiency enhancement than pure mineral thermal oil. The use of hybrid nanofluids has recently acquired growing attention. Bellos and Tzivanidis [25] evaluated the utilization of Al_2O_3–TiO_2 hybrid nanofluid dispersed on Syltherm 800 under typical operating conditions.

The majority of published works have been carried out by considering a uniform distribution of heat flux around the circumference of the receiver. However, in actual practice, the flux distribution over the receiver surface is highly non-uniform [26]. The induced stresses due to this uneven heat flux make the receiver tube deviate from the focal axis of the solar concentrator, thus rising optical losses. Wang et al. [3] proposed a method for designing a homogenizing reflector in conjunction with a conventional PTC that can enhance heat flux distribution around the circumference of the absorber tube wall. This study proposed an efficient step-by-step procedure incorporating the Monte Carlo ray-tracing (MCRT) and finite volume approach for the design procedure. Gong et al. [27] enhanced the flux distribution by using a secondary reflector (SR) as a flux homogenizing reflector. Bharti et al. [28] experimentally investigated the impact of the SRs on heat flux distribution over the receiver surface. They reported that with the use of parabolic shaped SRs, the output temperature of the working fluid was increased. The results showed that the maximum thermal efficiency could be improved by 6.5% for a parabolic secondary reflector as compared to that of a PTC without an SR. Rodriguez-Sanchez and Rosengarten [29] presented a theoretical analysis of a parabolic trough with a secondary flat mirror. The size and configurations of the system as obtained by the study reported increases close to 80% in the concentration ratio. An elliptical cavity receiver has been designed by Cao et al. [30]. Many SRs contribute to increased thermal losses by contacting the hot receiver, while many others leave an intended gap between the reflector and the receiver and suffer from larger optical losses. Wang et al. [31] conducted an optical–fluid–thermal–mechanical evaluation of a parabolic trough receiver, demonstrating the comparison of the thermal stress distribution of a parabolic trough receiver without and with a secondary reflector. A coupled MCRT–finite volume method (FVM)–FEM model is used to study supercritical CO_2 as the HTF. They found that under the tested conditions, uniform heat flux distribution due to the secondary reflector lowered the thermal stress from 50 MPa to 10 MPa. Tang et al. [32] recently proposed a design approach for balancing the heat flux around the receiver surface by optimizing the receiver location. Uzair and Rahman [33] developed a ray-tracing technique for evaluating the intercept factor of a beam-down PTC while considering the shading effect of the secondary reflector on the primary concentrator. In the majority of SR investigations, the position of the receiver tube is moved downward away from the focal axis of the primary collector, and an SR is mounded over the tube.

The design of a PTC with an SR faces two tasks: the determination of the desirable position of the receiver tube with respect to the focal axis of the primary reflector, and the other is the decision on the secondary reflector size and location. Applying a secondary reflector without a well-designed configuration can result in a more severe non-uniform heat flux distribution than the conventional collector and even structural failure of the receiver tube. The detailed literature reveals that there are no well-established design procedures for determining the size and location of the secondary reflector and the modified position of the receiver tube for a particular PTC for maximum uniformity of the heat flux. Therefore, this study investigates the application of a novel secondary parabolic reflector to homogenize the concentrated solar flux distribution on the receiver tube to achieve a uniform flux distribution over the surface. MCRT numerical analysis has been conducted to analyze the effect of the receiver tube and SR positions on the system's heat flux distributions and output power. For this, the distribution of solar flux over the surface of the absorber tube and the output power of the PTC has been simulated and determined by Tonatiuh software in different configurations.

2 Physical Model Description of Parabolic Trough Collector

A schematic model of the PTC with a parabolic SR is shown in Fig. 2. Solar radiations reflected by the main reflector are focused on the lower circumference of the receiver and the radiations that deviate from the tube are re-reflected by the SR on the upper circumference of the tube. The SR practically enhances the distribution of heat flux over the surface of the absorber tube when the system is installed at the desired configurations. The geometric parameters of the primary collector and receiver tube are listed in the Table 1. To study the effect of receiver tube position on the heat flux distribution over the receiver tube surface, the following changes are made: (1) receiver tube is moved down to different positions from the focal axis of the primary collector and (2) receiver tube is moved upward to different positions from the focal axis of the primary collector. Based on the new locations of the receiver, the focal length and width of the SR are determined by using the following formulas:

$$W_{SR} = \tan(\phi_{rp})[SRL - F - h] \tag{1}$$

$$h = \frac{W_{SR}^2}{16f} \tag{2}$$

The position of the SR concerning the receiver tube is fixed in such a way that its focal axis will be lying on the axis of the tube. For studying the downward misalignment of the receiver tube, three positions (z) such as 2.35 m, 2.3 m, and 2.25 m are considered. Similarly, three positions (z) such as 2.45 m, 2.5 m, and 2.55 m are considered for studying the upward misalignment of the receiver tube.

3 The Optical Model of Parabolic Trough Collector

The optical model of different configurations and the analysis of the PTC system have been carried out using MCRT simulations. In the past years, the MCRT method for analyzing the optical performance of CSPs has generally been followed because it is more powerful and adaptable [34–37]. Many other researchers have analyzed the solar–thermal energy exchange process of CSP systems using the MCRT method [38–40].

The ray-tracing tool, Tonatiuh, is used for the optical simulation. Tonatiuh is an MCRT-based, open-source, optical simulation tool developed by National Renewable Energy Centre of Spain (CENER) for all types of solar concentrators [36]. The most

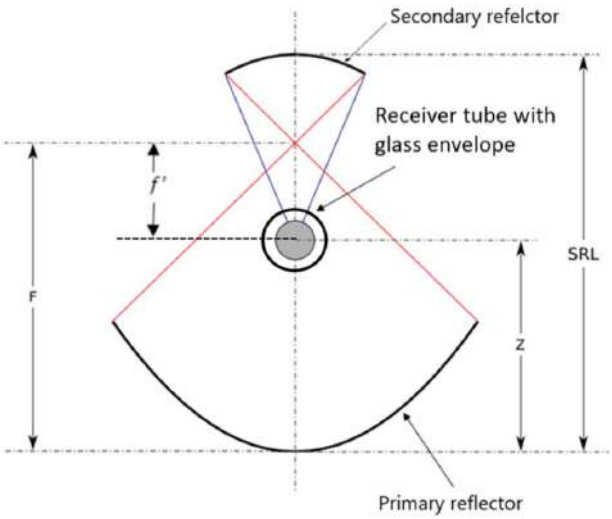

Fig. 2 Schematic diagram of PTC with secondary reflector

Table 1 Geometric parameters of primary collector and receiver

Sl. no.	Item	Numerical value
1	Aperture width (m)	8
2	Length of the collector (m)	5
3	Focal length (m)	2.4
4	Rim angle (deg)	80
5	Mirror reflectivity (primary and secondary)	0.97
6	Receiver tube diameter (m)	0.07
7	Glass cover diameter (m)	0.1

accurate and usually established sunshape Buie model is available with Tonatiue, and the model possesses axial as well as central symmetry [41]. According to this model, the distribution of terrestrial solar flux is given, as shown in Eq. (3)

$$\hat{L}_{Buie}(\phi) = \begin{cases} \dfrac{\cos 326(\phi)}{\cos 308(\phi)}, & 0 \le \phi \le \phi_{disc} \\ e^{\chi}(10^3\phi)^{\gamma}, & \phi_{disc} < \phi \le \phi_{aureole} \end{cases} \tag{3}$$

where ϕ is the radial angular displacement, η and γ are power functions of the circumsolar ratio. The annual averaged angular width of the solar disk, $\phi_{disc} \approx 4.65 \times 10^{-3}$ radians and the angular extent of the aureole, and $\phi_{aureole} \approx 43.6 \times 10^{-3}$ radians [42]. In this analysis, the reflectance of the reflectors has been taken as 0.98 and the absorptance of the absorber as 0.98. Beam irradiation of 1000 W/m^2 and a circumsolar ratio of 0.02 is considered for the simulation. With this model, the effect of geometric variations, such as the receiver tube position and secondary reflector geometry, on the heat flux distribution and power output can be studied. Tonatiuh simulates the incidence and reflection of solar rays and quantifies the energy flux that reaches the absorber surface. Here, the refractive component of the glass envelope is defined using two refractive surfaces. The optical properties, including absorption, reflection, transmittance, and refractive index, are defined at each side using

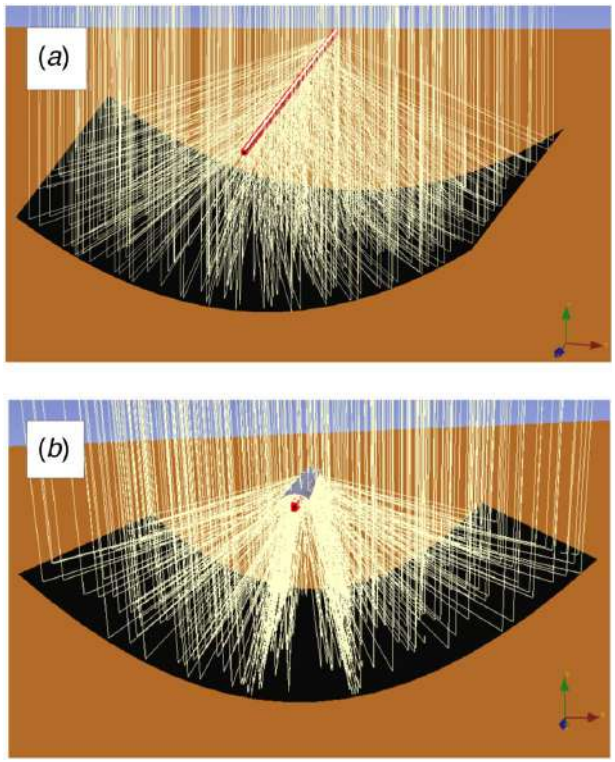

Fig. 3 Ray-tracing numerical simulation in Tonatiuh: (*a*) without SR and (*b*) with SR

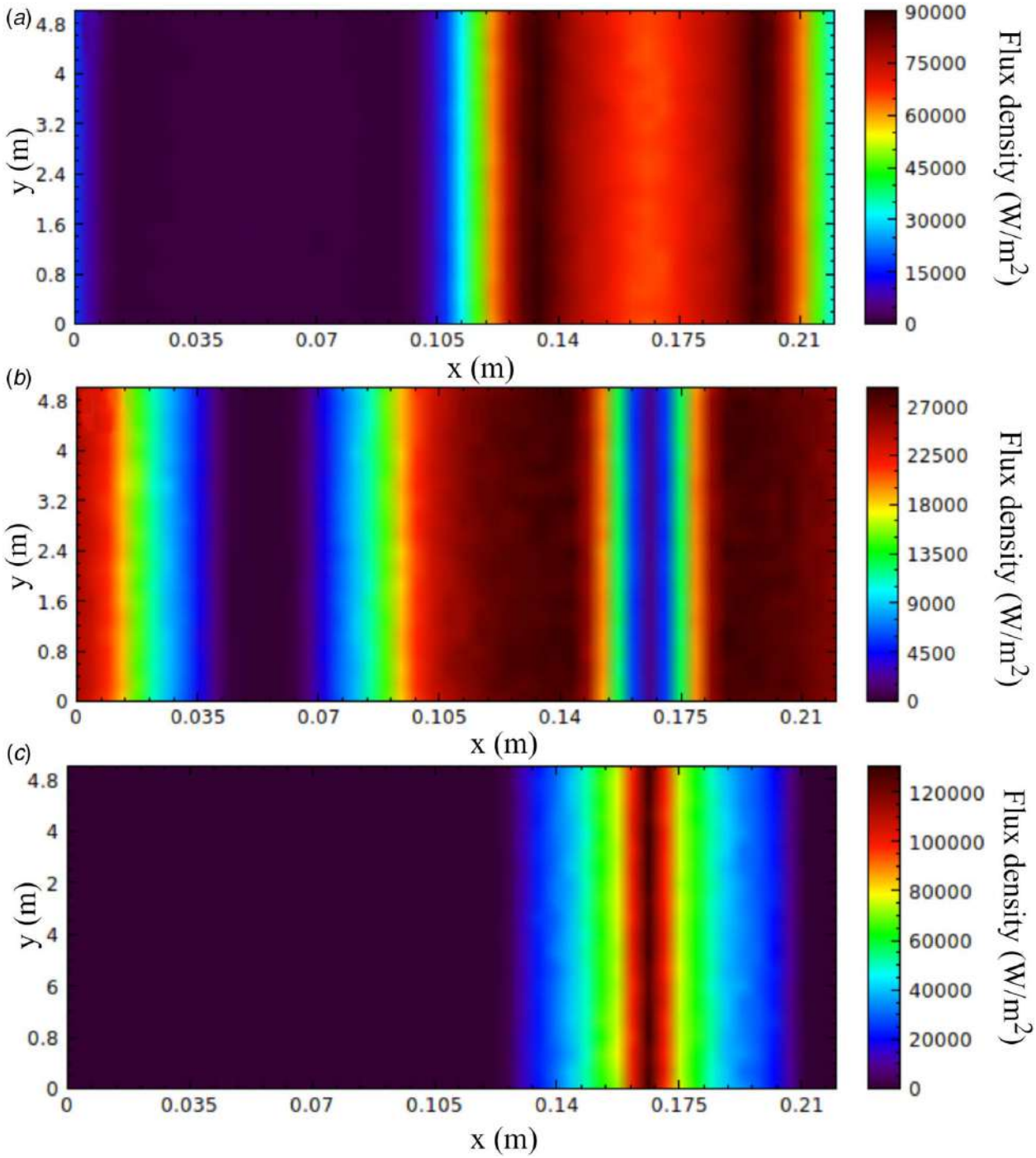

Fig. 4 Flux distribution (W/m^2) on the receiver tube wall: (*a*) receiver at focal axis without SR, (*b*) receiver below the focal axis with SR ($Z = 2.35$ m), and (c) receiver above the focal axis with SR ($Z = 2.55$ m)

the basic refractive material in Tonatiuh software. The transmissivity is assumed as 0.94 with a refractive index of 1.000277 in the airside and 1.5 in the evacuated space. Simulation of the MCRT optical models are set up and solved by the statistics, randomized trials and numerical approach of the Tonatiuh software.

4 Results and Discussion

The uniformity of heat flux distribution over the receiver tube and the power output of the PTC with an SR has been numerically studied by using Tonatiuh software. The receiver position and SR size have significantly affected the uniformity and power output. The results are presented for two cases: (i) PTC with the receiver tube mounted below the focal axis and (ii) receiver tube positioned above the focal axis. For each case, three SR locations have been investigated. Then, these results are compared with the outputs of a PTC with the receiver position identified by the geometrical study of the PTC.

4.1 MCRT Simulation. In order to calculate the distribution of solar heat flux over the receiver tube, a simulation with Tonatiuh has been conducted. The geometrical parameters of the primary concentrator and receiver tube are shown in Table 1, along with the different receiver positions and SR parameters, as discussed in

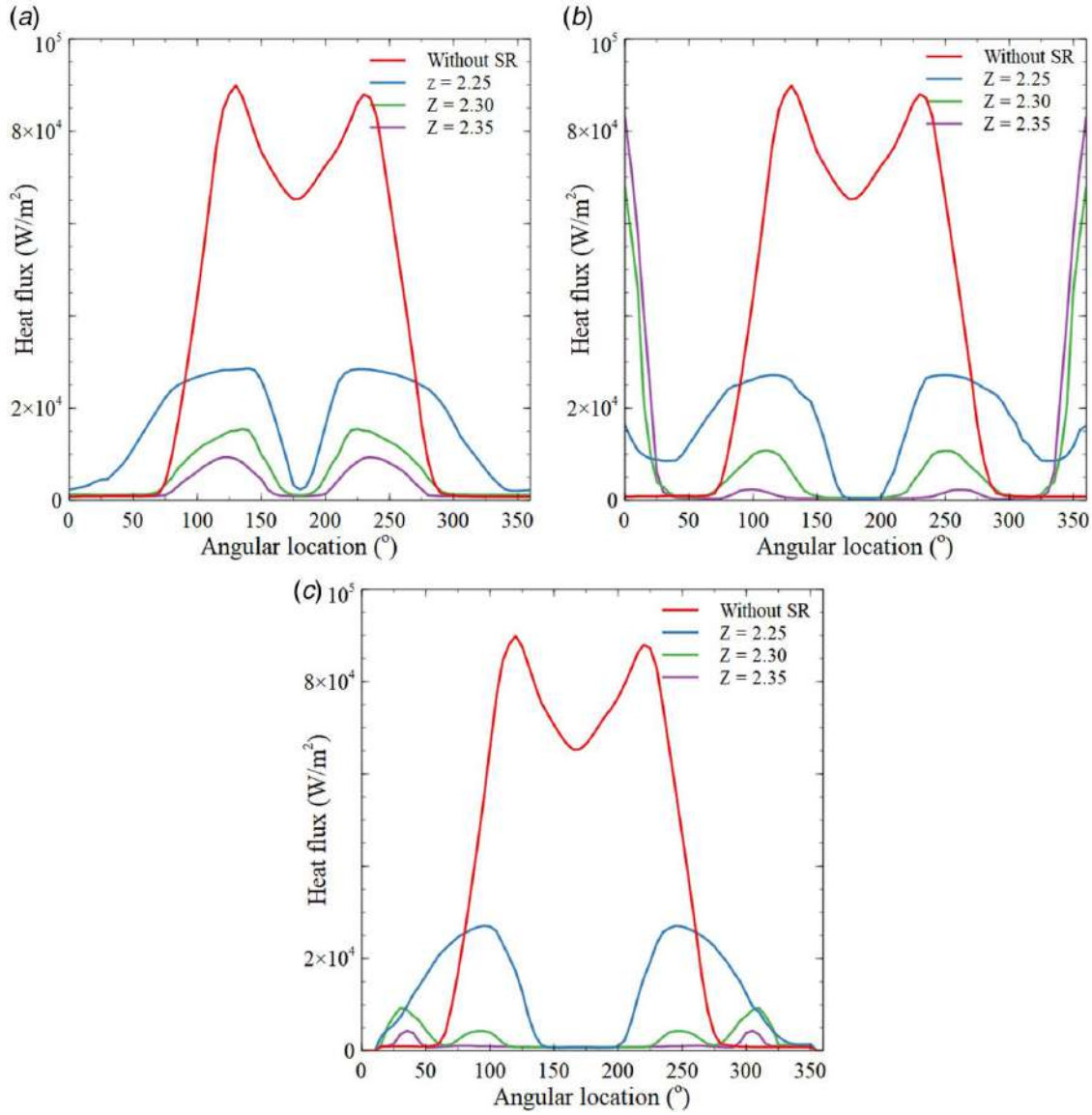

Fig. 5 Heat flux distribution for *z* below the focal axis: (*a*) SRL = 2.55 m, (*b*) SRL = 2.65 m, and (c) SRL = 2.75 m

Sec. 2. In the optical modeling, the sun shape is specified as the Buie model with one million beam radiations and 10^4 ray intersections, but to show a clear picture of the path of rays, 500 rays are used as shown in Figs. 3(*a*) and 3(*b*). As shown in Fig. 3(*a*), when the receiver tube is mounted on the exact focal axis, the entire reflected radiations are reflected into the bottom periphery of the tube. The receiver will fall under unequal intense solar radiation flux. While when the receiver is shifted down from the focal axis, and an SR is provided over the tube, the entire circumference of the tube is subjected to concentrated radiation as illustrated in Fig. 3(*b*), which leads to a more uniform distribution of the solar radiation flux.

4.2 Heat Flux Distribution Analysis. Solar heat flux distribution on the receiver tube surface, when the tube is placed at the focal axis of the primary reflector, below the focal axis and above the focal axis is illustrated in Figs. 4(*a*)–4(*c*), respectively. The simulation result indicates that the heat flux distribution is highly non-uniform when the receiver tube is at the real focal axis, as shown in Fig. 4(*a*). Similar results can be seen in the other investigations related to PTC receivers [28,43]. From this figure, it can be observed that the receiver tube located at the exact focal axis is subjected to a concentrated solar flux on the lower half. In contrast, the upper half is subjected to non-concentrated direct beam radiations. In this case, the peak heat flux is of the order of 90,000 W/m^2 and there is a large heat flux gradient between the bottom and upper portions of the receiver surface. By positioning the receiver tube downward and providing an SR, the part of radiations that could not reach the receiver tube can be reflected on the upper circumference of the tube by the SR. Accordingly, the distribution of heat flux over the receiver becomes homogeneous with a decreased gradient of flux (peak heat flux ≈ 27,000 W/m^2) as shown in Fig. 4(*b*). On the other hand, when the receiver is positioned above the focal axis, the majority of the reflected radiations pointed to a small area of the bottom surface of the tube. This results in a highly uneven distribution of heat flux with a severe peak heat flux of the order of 120,000 W/m^2 as shown in Fig. 4(*c*). This peak heat flux leads to local hot spots on the absorber wall and should be kept below safe levels to avoid receiver tube failures.

Figure 5 depicts the distribution of heat flux on the surface of the receiver tube when the tube is positioned at various positions (z) below the focal axis for various secondary reflector locations (SRL). The heat flux distribution on the PTC receiver tube without a secondary reflector, when the tube is positioned at the

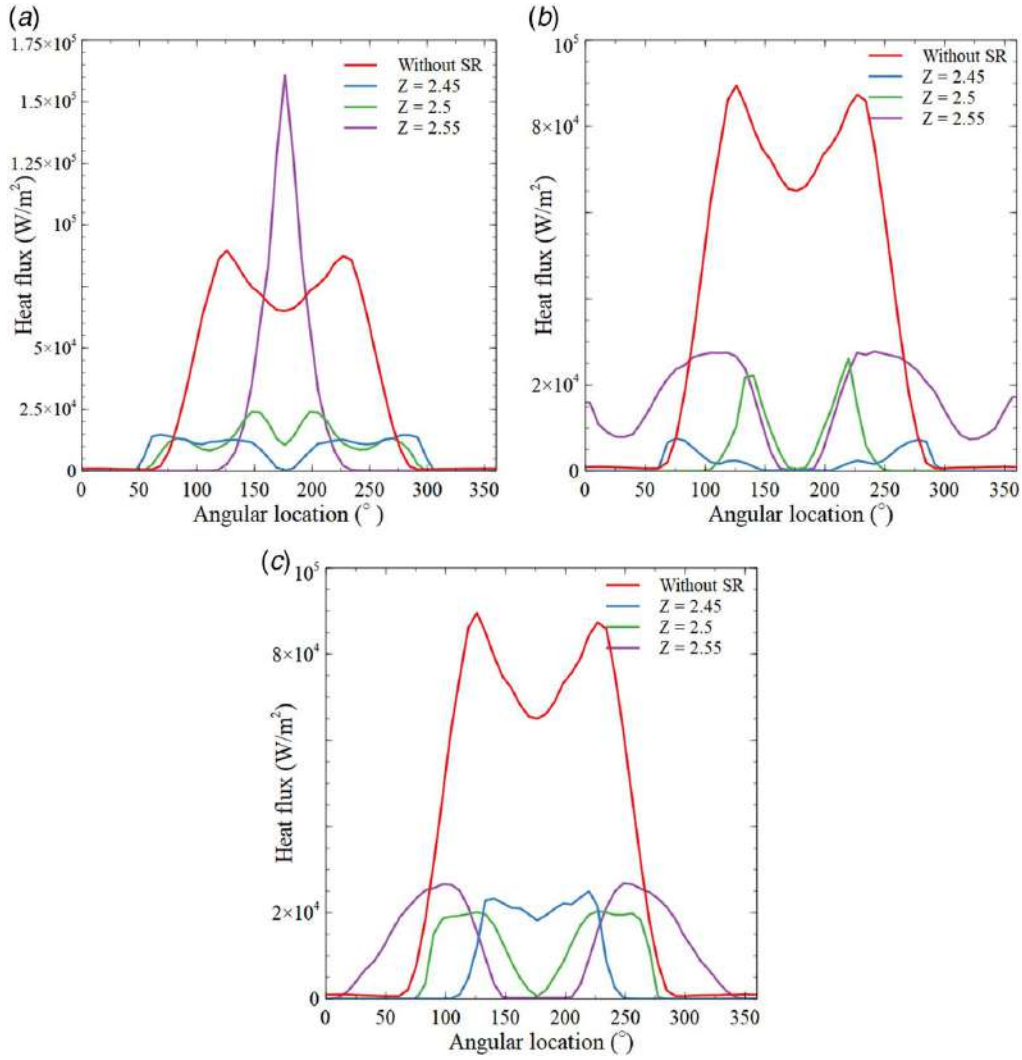

Fig. 6 Heat flux distribution for z above the focal axis: (*a*) SRL = 2.60 m, (*b*) SRL = 2.65 m, and (*c*) SRL = 2.75 m

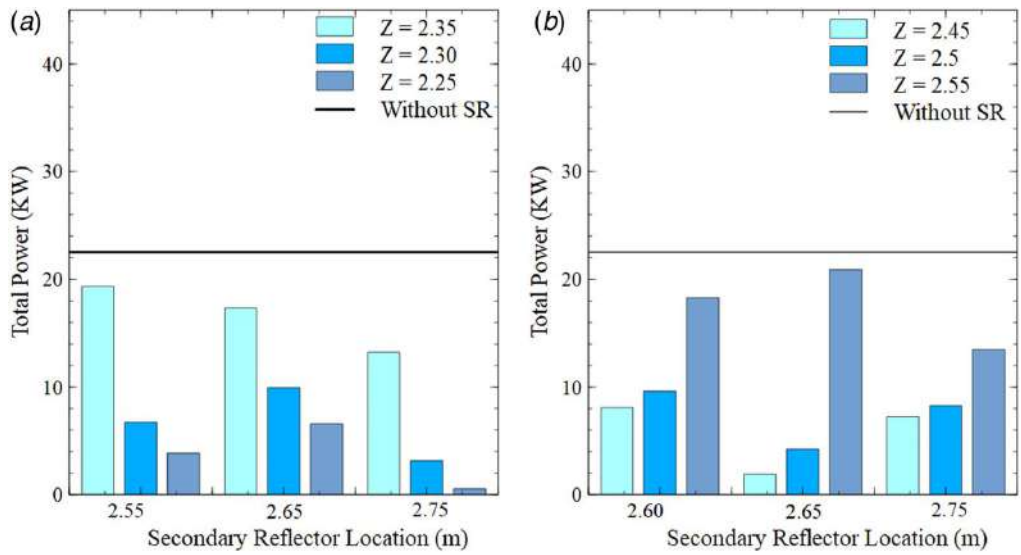

Fig. 7 Power output of the PTC: (*a*) receiver positioned below the focal axis and (*b*) receiver positioned above the focal axis

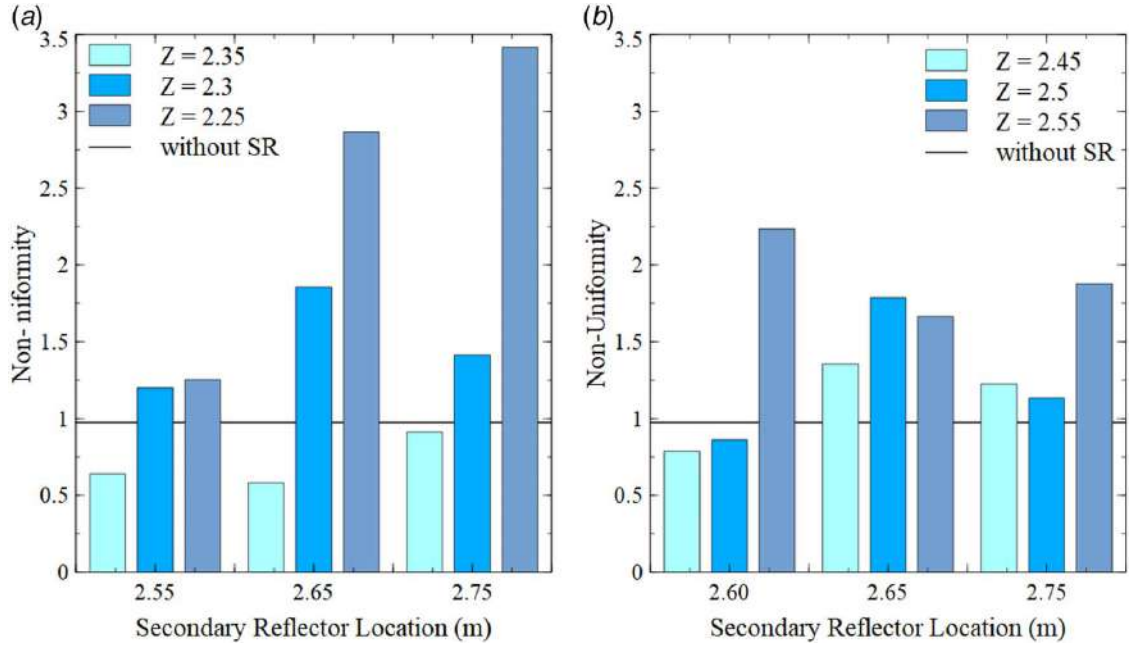

Fig. 8 Non-uniformity of heat flux distribution: (*a*) receiver positioned below the focal axis and (*b*) receiver positioned above the focal axis

focal axis of the main concentrator, is also shown for comparison in Figs. 5(*a*)–5(*c*). The simulation results show that the peak heat flux is about 89,556 W/m^2 when the receiver is placed at the focal axis of the primary collector without using an SR.

The heat flux drop in the center is due to the shading effect of the SR, which is in accordance with the width of the SR. The flux distribution is more flattened by providing the secondary reflector, as shown in Figs. 5(*a*)–5(*c*). When the receiver is away from the focal axis (nearer to the primary reflector), the peak flux is getting reduced and hence the flux gradient. This homogeneous flux distribution is due to the redistribution of the solar radiation flux by the SR and can enhance the reliability and longer service life of the PTC receiver. Figure 6 compares the heat flux distribution when the receiver tube is positioned at the exact focal axis and positioned at different positions above the focal axis with an SR. As shown in Fig. 6(*a*), the peak heat flux is pointed to a very high value, around 1.61×10^5 W/m^2. This extreme heat flux in a very small area of the absorber will cause large circumferential temperature differences and even structural failure of the PTC receiver. The axisymmetric peaks seen in Figs. 5 and 6 correspond to the highest flux values on the receiver tube surface due to the reflected rays from the primary concentrator. However, a third peak has been observed in some configurations that made the heat distribution curve asymmetrical. This asymmetrical flux distribution is evident from Fig. 5(*b*) (SRL = 2.65 m and Z = 2.25 m) for the PTC when the receiver tube is placed below the focal axis of the primary concentrator. This extra peak is occurred mainly due to the reflected rays from the secondary reflector. This implies that the receiver tube position and secondary reflector configuration have some remarkable effects on heat flux distribution and local hotspot formation. These negative aspects can be avoided only with the proper geometric design of the receiver position and secondary reflector.

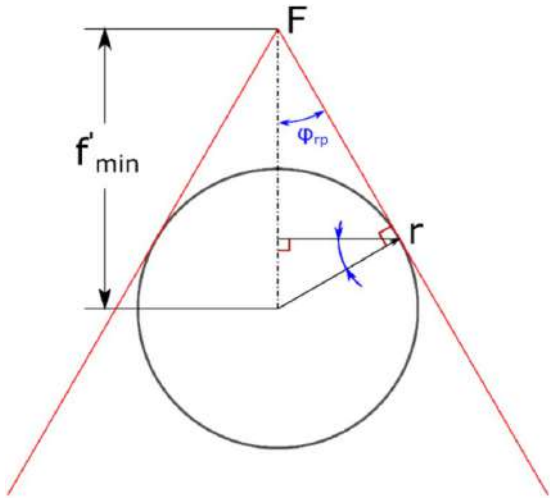

Fig. 9 Geometry to decide the desirable location of the receiver tube

4.3 Power Output and Uniformity of Heat Flux Distribution. This study has also investigated the power output from the PTC system and the non-uniformity of heat flux distribution over the receiver wall for different configurations. A substantial decrease in power output is observed for all the configurations examined compared to that of a conventional PTC with the receiver at its exact focal axis as depicted by Figs. 7(*a*) and 7(*b*). One of the reasons for this reduction in output power is the shadow projected from the SR on the primary concentrator. Therefore, in addition to the location of the secondary reflector, it is clear that the width of the SR needs to be carefully designed to take into account the maximum output power with better heat flux distribution.

From the results, when the receiver tube is moved down, the power output decreases as the receiver tube's deviation increases with respect to the exact focal axis of the primary reflector (Fig. 7(*a*)). On the other hand, as the receiver tube moves up from the focal axis, the power output increases for the three positions of the secondary reflector considered, as illustrated in Fig. 7(*b*). When the receiver is nearer to the focal axis, entire heat flux is pointed to a small area, as depicted in Fig. 6(*a*), which leads to poor conversion of solar energy to the receiver. Again, it is observed that for a multi-reflector PTC system, the SR position is a significant parameter in power output.

The non-uniformity of heat flux distribution for various configurations is illustrated in Figs. 8(*a*) and 8(*b*). It has been observed that the results are mixed for all the cases analyzed. In some examined

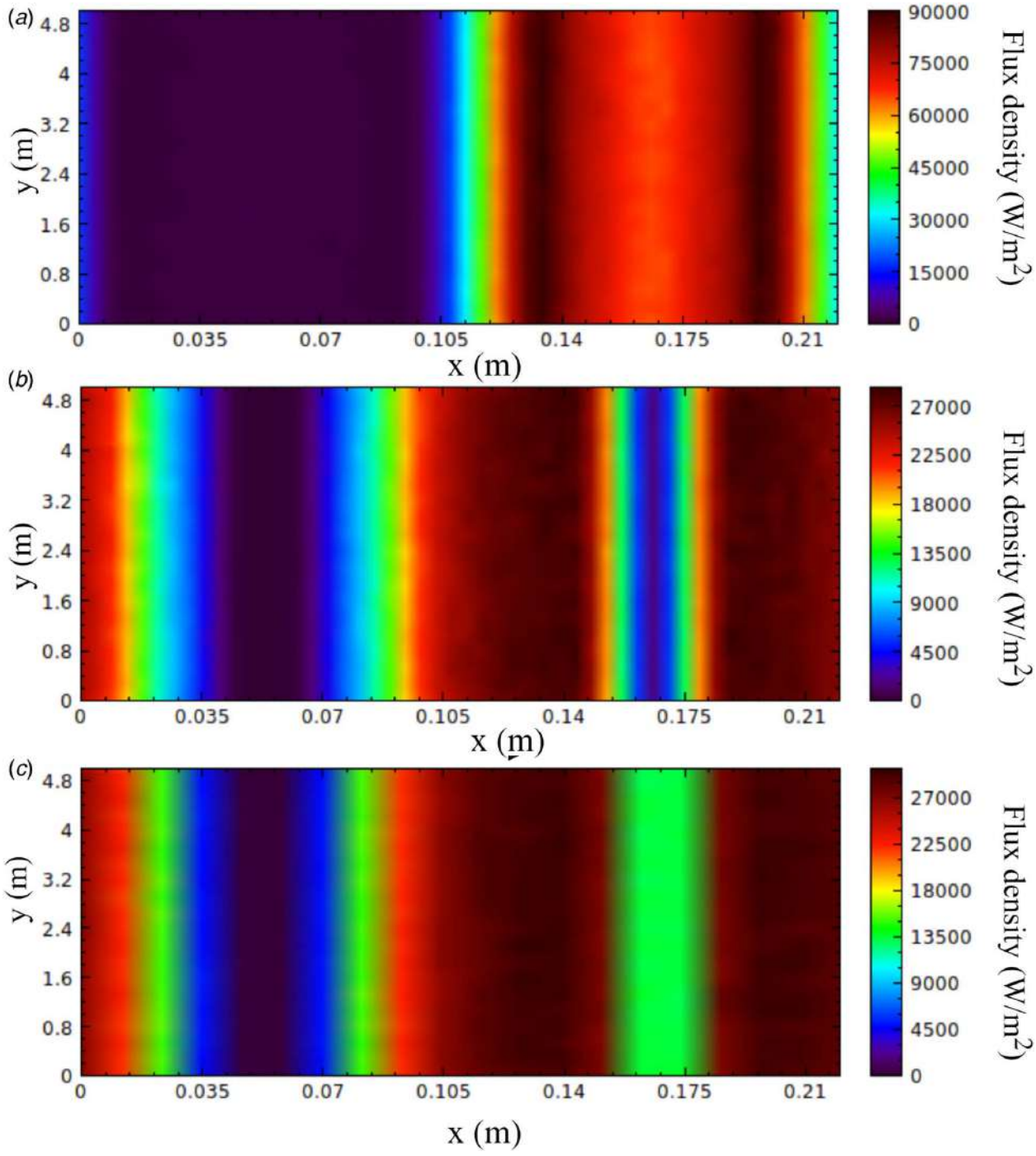

Fig. 10 Flux distribution (W/m^2) around receiver: (*a*) without SR, (*b*) $z = 2.35$ m, and (c) $z = 2.3645$ m

cases, the uniformity is better as compared to that of the conventional PTC, while in other cases, it is worse.

From Figs. 7 and 8, combined higher output power and a smaller non-uniformity are obtained at the receiver positions where it is located below the focal axis. In both cases, the comparative output power is obtained, but the non-uniformity of the heat flux distribution can seem to be lesser when the position of the receiver tube is below the focal axis (at $z = 2.35$ m).

Among all configurations, the most desirable parameters considering uniform heat flux distribution are $z = 2.35$ m and SRL = 2.55 m, with a total output power of 18.4 kW and a non-uniformity of 0.64. However, the output power of this configuration is found to be less than 4.305 kW, as compared to that of the PTC without the secondary reflector.

Since uneven heat flux distribution can induce significant thermal stress and even absorber tube failure [10], a collector needs to be developed to provide maximum power output with better distribution of heat flux. It is clear from Figs. 8(*a*) and 8(*b*) that for both cases, the important key factor that influenced the heat flux distribution is the distance, f', of the receiver tube from the focal point. Therefore, a geometric study has been conducted to determine the desirable position of the receiver tube with respect to the focal axis of the primary reflector. Accordingly, the minimum deviation of the receiver position from the exact focal point of the main concentrator is determined by taking into account the position at which the radiations reflected from the trough aperture edge rendered tangential to the absorber, as shown in Fig. 9.

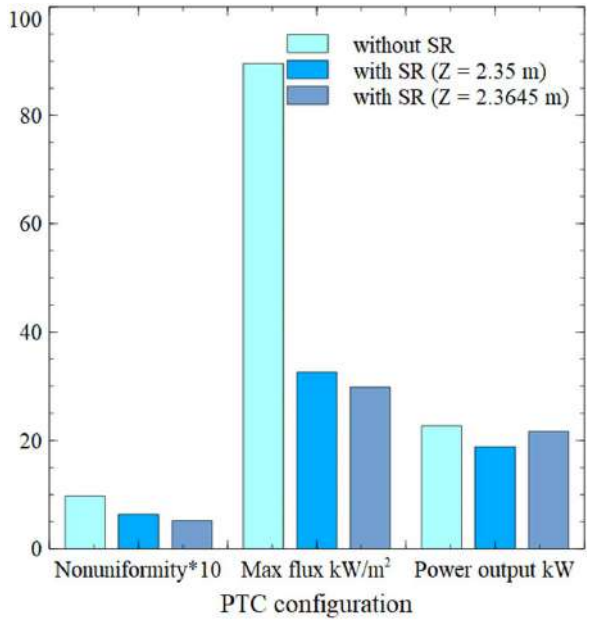

Fig. 11 Comparison of Tonatiuh simulation results

The desirable receiver position, as obtained based on the geometry by considering the above-said condition, is proposed as shown in Eq. (4).To reduce the losses because of blocking of direct solar beams on the primary reflector, the width of the secondary reflector is also limited to 5% of the aperture of the primary concentrator

$$f' = \frac{r}{\sin \phi_{rp}} \tag{4}$$

Based on these PTC configurations, ray-tracing analysis has been further carried out using Tonatiuh software (where $z = 2.3645$ m and $W_{SR} = 0.4$ m). Figures 10(*a*)–10(*c*) show the distribution of solar heat flux on the receiver's surface that went through simulation with Tonatiuh software for a PTC without SR, with an SR and tube at $z = 2.35$ m, and with an SR and tube at $z = 2.3645$ m, respectively. When $z = 2.3645$ m, the results of the ray-tracing

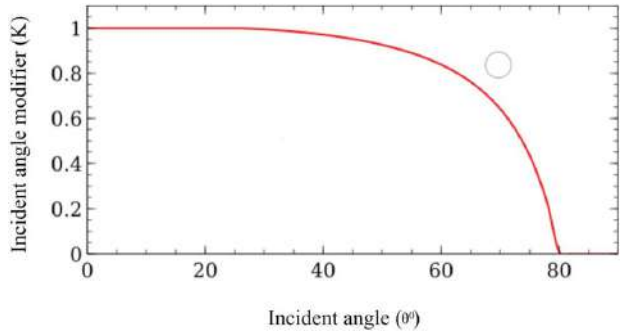

Fig. 12 Intercept factor for the proposed PTC

analysis showed that the distribution of heat flux around the receiver is more uniform (Fig. 10(*c*)) than that in other results. The highest flux in this configuration was 29.803 kW/m^2, with an output power of 21.648 kW, resulting in a lower non-uniformity value of 0.5176, indicating improved heat flux distribution.

A comparison of results for the three configurations, namely, PTC without SR, PTC with SR and $z = 2.35$ m, and the PTC with the configurations obtained by geometrical analysis is illustrated in Fig. 11. The non-uniformity of heat flux distribution of the PTC without SR, with SR and $z = 2.35$ m, with SR and $z = 2.3645$ m is 0.9757, 0.64, and 0.5176, respectively. From the results, the non-uniformity of heat flux on the receiver tube of the PTC with the desirable configuration as obtained from the geometrical study is lesser among the considered conditions. It can be observed that the maximum heat flux in the receiver without an SR is extremely high, which has a peak value of about 89.5 kW/m^2. This leads to a large temperature gradient and high thermal stresses, which is the main reason for the structural failure of PTC receivers [3].

Moreover, it is revealed that the peak heat flux and eventually the temperature gradient could substantially be reduced in the PTC with an SR, as shown in Fig. 11. The power output of the PTC without SR is recorded as 22.705 kW, and for a PTC with SR ($z = 2.35$ m), it is 18.83 kW, as illustrated in Fig. 11. While the power output for the PTC with SR ($z = 2.3645$ m) is 21.648 kW, which showed only a 4.83% reduction compared to the traditional PTC. The observed small reduction in power output with the use of SR is generally in agreement with the results that are presented by other works in

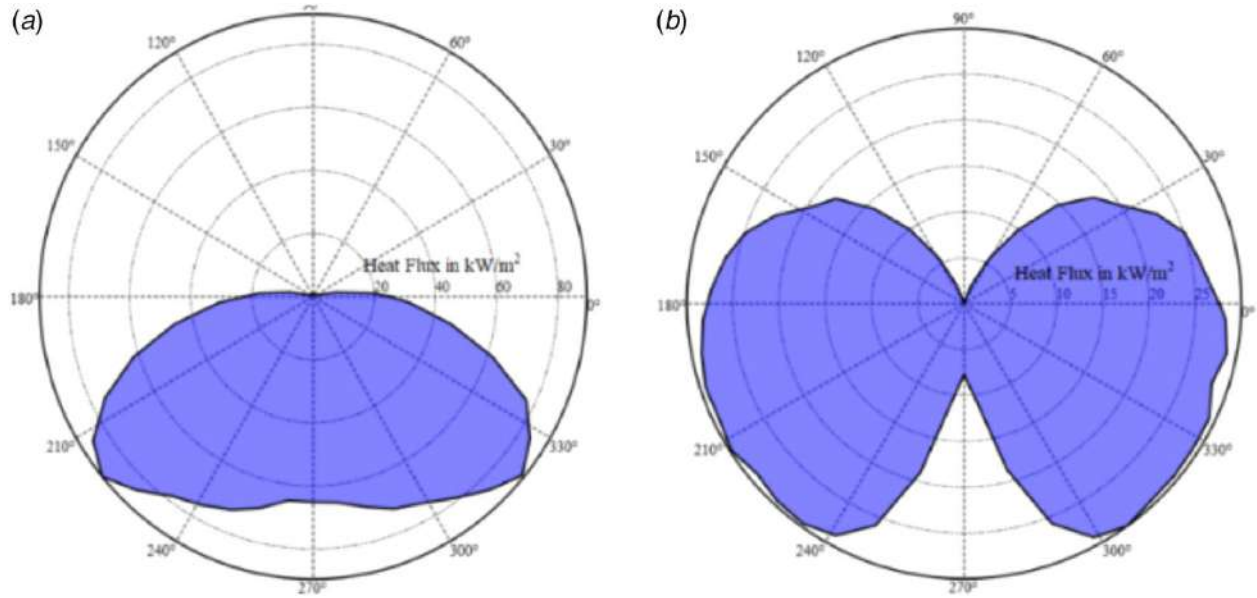

Fig. 13 Flux distribution around the receiver surface: (*a*) without SR and (*b*) with SR ($z = 2.3645$ m)

the literature [3]. It can also be noticed that by adding a secondary reflector, peak heat flux is decreased from 88.8 kW/m^2 to 27.4 kW/m^2. Moreover, the incident angle modifier (K) of the proposed system is analyzed by considering the proposed PTC is stationary. It is defined as the ratio of radiation incident at some incident angle θ to that at normal incidence. The relation of K is obtained as follows:

$$K = 1 + \frac{0.00105 \times \theta - 0.00004 \times \theta^2}{\cos \theta} \tag{5}$$

The K value is plotted in Fig. 12. It is evident from the figure that a value close to unity for a broad range up to 20 deg suggests that the proposed system can operate effectively for a wide range of incident angle.

In actual practice, this higher value of power output of the conventional PTC is not easily achievable because of the thermal distortion of the receiver tube due to the extreme flux gradient. Thermal bending also reduces the reception of solar radiation on the receiver tube [44]. Furthermore, due to the profile errors on the primary collector, a significant portion of the reflected radiations cannot reach the receiver tube. This might ultimately result in smaller power output than the PTC system with SR at most desirable configurations. On the other hand, for a PTC with an SR, lost radiations due to the bending of the tube and the profile errors on the primary reflector can be re-reflected onto the tube using the SR. Additionally, the use of an SR reduces the need for high sensitivity of the tracking system since the SR is able to control the solar radiations that do not reach directly to the receiver from the primary concentrator [45]. Figures 13(*a*) and 13(*b*) illustrate the distribution of heat flux around the circumference of the absorber tube without and with the SR, respectively, obtained from the Tonatiuh ray-tracing analysis.

From Fig. 13, it can also be observed that the PTC with SR at its most desirable configuration could significantly homogenize the heat flux over the receiver. As a result, the circumferential heat gradient and the local hot spot could be reduced significantly. Under the conditions investigated in the present study, although the output power decreased from 22.705 kW to 21.705 kW, the flux gradient decreased significantly, and the non-uniformity of flux distribution reduced from 0.9757 to 0.5176.

5 Conclusions

In this study, the influence of circumferential solar heat flux distributions on the receiver tube of a PTC has been numerically investigated for three different conditions viz. without an SR, for different receiver tube positions with an SR and using the configuration as obtained from the geometric study. The results of Tonatiuh software reveal that the circumferential heat flux gradient on the receiver tube for the configuration obtained through the geometric study is significantly better than the case without an SR. It can be noticed that, at certain receiver tube locations, heat flux distribution is worse when SR is used. This reveals that applying a secondary reflector without a well-designed configuration can result in a more severe non-uniform heat flux distribution than the conventional collector and even structural failure of the receiver tube. This study proposed a geometric approach with suitable assumptions for the receiver location and secondary reflector size for maximum heat flux distribution, and it is confirmed through the MCRT results. Under the conditions investigated in this work, although the output power decreased by 4.83%, the flux gradient reduced significantly, and the non-uniformity of flux distribution is reduced by a factor of 1.87. It can also be found that the heat flux gradient is reduced by 70% by adding a secondary reflector. From the results, it can be concluded that the heat flux distribution can be homogenized by moving the receiver toward the primary collector and adding an SR with the most desirable geometry and configurations. The gradient of heat flux can be kept below the safe level to ensure the longer service life of the absorber tube with a negligible reduction in power output.

Conflict of Interest

There are no conflicts of interest.

Data Availability Statement

The datasets generated and supporting the findings of this article are obtainable from the corresponding author upon reasonable request.

Nomenclature

f = focal length of secondary reflector (m)
h = height of secondary reflector (m)
r = radius of the receiver tube (m)
F = focal length of the primary reflector (m)
Z = distance between the primary collector and the receiver tube (m)
W_{SR} = width of the secondary reflector (m)
f' = distance to receiver center from the focal point (m)

Greek Symbols

η = function of sunshape for a given circumsolar ratio
ϕ = radial angular displacement (radian)
ϕ_{rp} = rim angle of primary reflector (deg)
γ = function of the circumsolar ratio

References

[1] Ullah, K. R., Saidur, R., Ping, H. W., Akikur, R. K., and Shuvo, N. H., 2013, "A Review of Solar Thermal Refrigeration and Cooling Methods," Renewable Sustainable Energy Rev., **24**, pp. 499–513.
[2] Desai, N. B., and Bandyopadhyay, S., 2017, "Line-Focusing Concentrating Solar Collector-Based Power Plants: A Review," Clean Technol. Environ. Policy, **19**(1), pp. 9–35.
[3] Wang, K., He, Y., and Cheng, Z., 2014, "A Design Method and Numerical Study for a New Type Parabolic Trough Solar Collector With Uniform Solar Flux Distribution," Sci. China Technol. Sci., **57**(3), pp. 531–540.
[4] He, Y. L., Wang, K., Qiu, Y., Du, B. C., Liang, Q., and Du, S., 2019, "Review of the Solar Flux Distribution in Concentrated Solar Power: Non-uniform Features, Challenges, and Solutions," Appl. Therm. Eng., **149**, pp. 448–474.
[5] Minaeian, A., Alemrajabi, A., Chavoshi, M., Mostafaeipour, A., and Seifi, Z., 2020, "Effect of Secondary Reflector on Solar Flux Intensity and Uniformity of a Fresnel Concentrator," J. Renewable Sustainable Energy, **12**(3), p. 033703.
[6] Okafor, I. F., Dirker, J., and Meyer, J. P., 2014, "Influence of Circumferential Solar Heat Flux Distribution on the Heat Transfer Coefficients of Linear Fresnel Collector Absorber Tubes," Sol. Energy, **107**, pp. 381–397.
[7] Mwesigye, A., Bello-Ochende, T., and Meyer, J. P., 2014, "Heat Transfer and Thermodynamic Performance of a Parabolic Trough Receiver With Centrally Placed Perforated Plate Inserts," Appl. Energy, **136**, pp. 989–1003.
[8] Wu, Z., Lei, D., Yuan, G., Shao, J., Zhang, Y., and Wang, Z., 2014, "Structural Reliability Analysis of Parabolic Trough Receivers," Appl. Energy, **123**, pp. 232–241.
[9] Wang, K., He, Y. L., Xue, X. D., and Du, B. C., 2017, "Multi-objective Optimization of the Aiming Strategy for the Solar Power Tower With a Cavity Receiver by Using the Non-dominated Sorting Genetic Algorithm," Appl. Energy, **205**, pp. 399–416.
[10] Ibrar Hussain, M., Mokheimer, E. M. A., and Ahmed, S., 2017, "Optimal Design of a Solar Collector for Required Flux Distribution on a Tubular Receiver," ASME J. Energy Resour. Technol., **139**(1), p. 012006.
[11] Jaramillo, O. A., Borunda, M., Velazquez-Lucho, K. M., and Robles, M., 2016, "Parabolic Trough Solar Collector for Low Enthalpy Processes: An Analysis of the Efficiency Enhancement by Using Twisted Tape Inserts," Renewable Energy, **93**, pp. 125–141.
[12] Bellos, E., Tzivanidis, C., Antonopoulos, K. A., and Gkinis, G., 2016, "Thermal Enhancement of Solar Parabolic Trough Collectors by Using Nano Fluids and Converging-Diverging Absorber Tube," Renewable Energy, **94**, pp. 213–222.
[13] Huang, Z., Li, Z. Y., Yu, G. L., and Tao, W. Q., 2017, "Numerical Investigations on Fully-Developed Mixed Turbulent Convection in Dimpled Parabolic Trough Receiver Tubes," Appl. Therm. Eng., **114**, pp. 1287–1299.
[14] Ravi Kumar, K., and Reddy, K. S., 2009, "Thermal Analysis of Solar Parabolic Trough With Porous Disc Receiver," Appl. Energy, **86**(9), pp. 1804–1812.

[15] Wang, P., Li, J. B., Vafai, K., Zhao, L., and Zhou, L., 2017, "Thermo-Fluid Optimization of a Solar Porous Absorber With a Variable Pore Structure," ASME J. Sol. Energy Eng., **139**(5), p. 051012.
[16] Cheng, Z. D., He, Y. L., and Cui, F. Q., 2012, "Numerical Study of Heat Transfer Enhancement by Unilateral Longitudinal Vortex Generators Inside Parabolic Trough Solar Receivers,"," Int. J. Heat Mass Transfer, **55**(21–22), pp. 5631–5641.
[17] Okonkwo, E. C., Abid, M., and Ratlamwala, T. A. H., 2018, "Numerical Analysis of Heat Transfer Enhancement in a Parabolic Trough Collector Based on Geometry Modifications and Working Fluid Usage," ASME J. Sol. Energy Eng., **140**(5), p. 051009.
[18] Mwesigye, A., Bello-Ochende, T., and Meyer, J. P., 2016, "Heat Transfer and Entropy Generation in a Parabolic Trough Receiver With Wall-Detached Twisted Tape Inserts," Int. J. Therm. Sci., **99**, pp. 238–257.
[19] Desai, N. B., and Bandyopadhyay, S., 2015, "Integration of Parabolic Trough and Linear Fresnel Collectors for Optimum Design of Concentrating Solar Thermal Power Plant," Clean Technol. Environ. Policy, **17**(7), pp. 1945–1961.
[20] Xu, H., Li, Y., Sun, J., and Li, L., 2019, "Transient Model and Characteristics of Parabolic-Trough Solar Collectors : Molten Salt vs. Synthetic Oil," Sol. Energy, **182**, pp. 182–193.
[21] Chang, C., Sciacovelli, A., Wu, Z., Li, X., Li, Y., Zhao, M., Deng, J., Wang, Z., and Ding, Y., 2018, "Enhanced Heat Transfer in a Parabolic Trough Solar Receiver by Inserting Rods and Using Molten Salt as Heat Transfer Fluid," Appl. Energy, **220**, pp. 337–350.
[22] Sarkar, J., Ghosh, P., and Adil, A., 2015, "A Review on Hybrid Nano Fluids : Recent Research, Development and Applications," Renewable Sustainable Energy Rev., **43**, pp. 164–177.
[23] Kasaeian, A., Daviran, S., Azarian, R. D., and Rashidi, A., 2015, "Performance Evaluation and Nanofluid Using Capability Study of a Solar Parabolic Trough Collector," Energy Convers. Manage., **89**, pp. 368–375.
[24] Khakrah, H., Shamloo, A., and Hannani, S. K., 2017, "Determination of Parabolic Trough Solar Collector Efficiency Using Nanofluid: A Comprehensive Numerical Study," ASME J. Sol. Energy Eng., **139**(5), p. 051006.
[25] Bellos, E., and Tzivanidis, C., 2018, "Thermal Analysis of Parabolic Trough Collector Operating With Mono and Hybrid Nanofluids," Sustain. Energy Technol. Assess., **26**, pp. 105–115.
[26] Hachicha, A. A., Rodríguez, I., Capdevila, R., and Oliva, A., 2013, "Heat Transfer Analysis and Numerical Simulation of a Parabolic Trough Solar Collector," Appl. Energy, **111**, pp. 581–592.
[27] hu Gong, J., Wang, J., Lund, P. D., yi Hu, E., cheng Xu, Z., peng Liu, G., and shuai Li, G., 2020, "Improving the Performance of a 2-Stage Large Aperture Parabolic Trough Solar Concentrator Using a Secondary Reflector Designed by Adaptive Method," Renewable Energy, **152**, pp. 23–33.
[28] Bharti, A., Mishra, A., and Paul, B., 2019, "Thermal Performance Analysis of Small-Sized Solar Parabolic Trough Collector Using Secondary Reflectors," Int. J. Sustainable Energy, **38**(10), pp. 1002–1022.
[29] Rodriguez-Sanchez, D., and Rosengarten, G., 2015, "Improving the Concentration Ratio of Parabolic Troughs Using a Second-Stage Flat Mirror," Appl. Energy, **159**, pp. 620–632.
[30] Cao, F., Li, Y., Wang, L., and Zhu, T. Y., 2016, "Thermal Performance and Stress Analyses of the Cavity Receiver Tube in the Parabolic Trough Solar Collector," IOP Conf. Ser. Earth Environ. Sci., **40**, p. 012067.
[31] Wang, K., Zhang, Z.-D., Li, M.-J., and Min, C. H., 2021, "A Coupled Optical-Thermal-Fluid-Mechanical Analysis of Parabolic Trough Solar Receivers Using Supercritical CO_2 as Heat Transfer Fluid," Appl. Therm. Eng., **183**, p. 116154.
[32] Tang, X. Y., Yang, W. W., Yang, Y., Jiao, Y. H., and Zhang, T., 2021, "A Design Method for Optimizing the Secondary Reflector of a Parabolic Trough Solar Concentrator to Achieve Uniform Heat Flux Distribution," Energy, **229**, p. 120749.
[33] Uzair, M., and Rehman, N. U., 2021, "Intercept Factor for a Beam-Down Parabolic Trough Collector," ASME J. Sol. Energy Eng., **143**(6), p. 061002.
[34] Wang, X., Luo, S., Tang, T., Liu, X., and He, Y., 2019, "A MCRT-FVM-FEM Coupled Simulation for Optical-Thermal-Structural Analysis of Parabolic Trough Solar Collectors," Energy Procedia, **158**, pp. 477–482.
[35] Cheng, Z. D., He, Y. L., Cui, F. Q., Xu, R. J., and Tao, Y. B., 2012, "Numerical Simulation of a Parabolic Trough Solar Collector With Non-Uniform Solar Flux Conditions by Coupling FVM and MCRT Method," Sol. Energy, **86**(6), pp. 1770–1784.
[36] Yuan, G., Fan, J., Kong, W., Furbo, S., Perers, B., and Sallaberry, F., 2020, "Experimental and Computational Fluid Dynamics Investigations of Tracking CPC Solar Collectors," Sol. Energy, **199**, pp. 26–38.
[37] Lüpfert, E., Pottler, K., Ulmer, S., Riffelmann, K. J., Neumann, A., and Schiricke, B., 2007, "Parabolic Trough Optical Performance Analysis Techniques," ASME J. Sol. Energy Eng., **129**(2), pp. 147–152.
[38] Cheng, Z. D., He, Y. L., Du, B. C., Wang, K., and Liang, Q., 2015, "Geometric Optimization on Optical Performance of Parabolic Trough Solar Collector Systems Using Particle Swarm Optimization Algorithm," Appl. Energy, **148**, pp. 282–293.
[39] Dong, X., Nathan, G. J., Sun, Z., Ashman, P. J., and Gu, D., 2016, "Secondary Concentrators to Achieve High Flux Radiation With Metal Halide Solar Simulators," ASME J. Sol. Energy Eng., **138**(4), p. 041001.
[40] Wu, Z., Li, S., Yuan, G., Lei, D., and Wang, Z., 2014, "Three-Dimensional Numerical Study of Heat Transfer Characteristics of Parabolic Trough Receiver," Appl. Energy, **113**, pp. 902–911.
[41] Chen, F., Li, M., and Zhang, P., 2015, "Distribution of Energy Density and Optimization on the Surface of the Receiver for Parabolic Trough Solar Concentrator," Int. J. Photoenergy, **2015**, pp. 1–10.
[42] Wang, Y., Potter, D., Asselineau, C. A., Corsi, C., Wagner, M., Caliot, C., Piaud, B., Blanco, M., Kim, J. S., and Pye, J., 2020, "Verification of Optical Modelling of Sunshape and Surface Slope Error for Concentrating Solar Power Systems," Sol. Energy, **195**, pp. 461–474.
[43] Reda, H. M., and Abdelylah, B., 2019, "Numerical Investigation and Solar Flux Distribution Analysis of Parabolic Trough Solar Collector by Adding Secondary Reflector," Instrum. Mes. Metrol., **18**(3), pp. 275–280.
[44] Tripathy, A. K., Ray, S., Sahoo, S. S., and Chakrabarty, S., 2018, "Structural Analysis of Absorber Tube Used in Parabolic Trough Solar Collector and Effect of Materials on Its Bending: A Computational Study," Sol. Energy, **163**, pp. 471–485.
[45] Bellos, E., and Tzivanidis, C., 2019, "Alternative Designs of Parabolic Trough Solar Collectors," Prog. Energy Combust. Sci., **71**, pp. 81–117.